The novel sphingosine 1-phosphate receptor AGR16 is coupled via pertussis toxin-sensitive and -insensitive G-proteins to multiple signalling pathways

Koichi GONDA*†, Hiroyuki OKAMOTO*‡, Noriko TAKUWA*, Yutaka YATOMI§, Hiroshi OKAZAKI‖, Takeshi SAKURAI¶, Sadao KIMURA**, Rannar SILLARD††, Kiyonori HARII† and Yoh TAKUWA*‖‡‡[1]

*Department of Molecular and Cellular Physiology, University of Tokyo Graduate School of Medicine, Tokyo 113–0033, Japan, †Department of Plastic and Reconstructive Surgery, University of Tokyo Graduate School of Medicine, Tokyo 113–0033, Japan, ‡Department of Vascular Surgery, University of Tokyo Graduate School of Medicine, Tokyo 113–0033, Japan, §Department of Laboratory Medicine, Yamanashi Medical University, Tamaho-cho, Yamanashi 408–3898, Japan, ‖Department of Cardiovascular Biology, University of Tokyo Graduate School of Medicine, Tokyo 113–0033, Japan, ¶Department of Pharmacology, Institute of Basic Medical Sciences, University of Tsukuba, Tsukuba, Ibaraki 305–0006, Japan, **Division of Cardiovascular Biology, Center for Biomedical Sciences, Chiba University Medical School, Chiba 260–0856, Japan, ††Department of Medical Biochemistry and Biophysics, Karolinska Institute, S-171 77 Stockholm, Sweden, and ‡‡Foundation for Advancement of International Science, Tsukuba, Ibaraki 305–0005, Japan

In the present study, we determined the agonist specificity and the signalling mechanisms of a putative sphingosine 1-phosphate (S1P) receptor, AGR16. In CHO cells transiently transfected with an AGR16 expression vector, but not in cells transfected with an empty vector, the addition of a low concentration of S1P (1 nM) caused an increase in the intracellular free Ca^{2+} concentration ($[Ca^{2+}]_i$) by mobilization of Ca^{2+} from both intra- and extra-cellular pools. To determine the spectrum of agonists for AGR16, we employed K562 cells, which in the naive state do not respond at all to either S1P or structurally related lipids with an increase in $[Ca^{2+}]_i$. In K562 cells stably expressing AGR16, S1P and sphingosylphosphorylcholine (SPC) dose-dependently increased $[Ca^{2+}]_i$ with half-maximal values of 3 nM and 100 nM respectively. In CHO cells stably expressing AGR16 (CHO-AGR16), but not in parental CHO cells, we observed specific binding of [^{32}P]S1P, which was displaced by unlabelled S1P and SPC. In CHO-AGR16 cells, but not in parental CHO cells, S1P stimulated the production of inositol phosphates and Ca^{2+} mobilization which was only 30% inhibited by pertussis toxin (PTX), different from the case of the recently identified S1P receptor EDG1. Also in CHO-AGR16 cells, but not in CHO cells, S1P at higher concentrations activated mitogen-activated protein kinase (MAPK) in a PTX-sensitive and Ras-dependent manner. S1P also induced the activation of two stress-activated MAPKs, c-Jun N-terminal kinase and p38, in a manner that was totally insensitive to PTX. In CHO-AGR16 cells, S1P induced stress-fibre formation, with an increase in myosin light chain phosphorylation, in a PTX-insensitive and Rho-dependent manner. S1P also induced an increase in the cellular cAMP content in CHO-AGR16 cells, which contrasts sharply with the case of EDG1. These results establish that the S1P receptor AGR16 is coupled via both PTX-sensitive and -insensitive G-proteins to multiple effector pathways.

Key words: adenylate cyclase, G-protein-coupled receptor, lysophospholipid, mitogen-activated protein kinase, phospholipase C.

INTRODUCTION

Accumulating evidence now indicates that the lysosphingolipids sphingosine 1-phosphate (S1P) and sphingosylphosphorylcholine (SPC) constitute a group of important extracellular lipid mediators [1–4]. Both S1P and SPC have been shown to regulate such diverse cellular functions as proliferation [5,6], migration [7,8] and cell shape change [9,10] in a variety of cell types. It was demonstrated previously [11–13] that S1P at high concentrations could act directly on intracellular Ca^{2+} stores to induce Ca^{2+} release. This observation, together with the finding that growth factors and other extracellular stimuli induce activation of sphingolipid metabolism leading to the production of S1P [8,14,15], suggested that S1P might act as an intracellular second messenger. However, subsequent studies have revealed that S1P and SPC activate multiple intracellular signalling molecules, including phospholipase C [8,16,17], phospholipase D [6,16], mitogen-activated protein kinase (MAPK)/extracellular-signal-regulated kinase (ERK) [8,18], protein kinase C (PKC) [19] and the K^+ [$I_{K(Ach)}$] channel [20]. Also, many of the lysosphingolipid-induced cellular responses were shown to be inhibited by pertussis toxin (PTX) pretreatment [8,16,21]. Moreover, it was demonstrated that the addition of S1P to culture medium, but not the intracellular injection of S1P, induced morphological changes in NIE-115 neuronal cells [9]. It was also reported that immobilized S1P covalently linked to glass particles was able to activate platelets [22]. These observations favour the view that lysosphingolipids exert many of their biological activities via cell-surface receptors [4]. Importantly, it was recently demonstrated [23] that S1P is present in the plasma at a readily detectable level,

Abbreviations used: ATF, activating transcription factor; $[Ca^{2+}]_i$, intracellular free Ca^{2+} concentration; EDG, endothelial differentiation gene; ERK, extracellular-signal-regulated kinase; GST, glutathione S-transferase; JNK, c-Jun N-terminal kinase; LPA, lysophosphatidic acid; MAPK, mitogen-activated protein kinase; MLC, 20 kDa myosin light chain; PKC, protein kinase C; PTX, pertussis toxin; SPC, sphingosylphosphorylcholine; S1P, sphingosine 1-phosphate.

[1] To whom correspondence should be addressed: Department of Molecular and Cellular Physiology, University of Tokyo School of Medicine, 7-3-1 Hongo, Bunkyo-ku, Tokyo 113, Japan (e-mail yohtakwa@m.u-tokyo.ac.jp).

implying physiological and pathophysiological roles for S1P as a first messenger.

The present study demonstrates that AGR16/H218/EDG5 (endothelial differentiation gene 5) [24,25], a member of EDG receptor family with a seven-transmembrane structure [26–28], is a functional receptor for S1P, with signalling characteristics clearly distinct from those of EDG1, the first S1P receptor identified [29–31]. We originally cloned AGR16 from rat aortic smooth muscle [24]. We have defined the intracellular signalling pathways activated by AGR16, and determined the ligand specificity of AGR16, by studying responses in mammalian cells (CHO and K562) transiently or stably transfected with an AGR16 expression vector. While this paper was in preparation, it was reported [32] that the overexpression of AGR16 in Jurkat T-cells and *Xenopus* oocytes conferred the ability to respond to S1P and SPC, with stimulation of serum-response-element-driven transcriptional activity and Ca^{2+} efflux respectively. However, other functional aspects of AGR16 as the receptor for S1P, as well as the agonist specificity of AGR16, have not been elucidated.

It was demonstrated recently that another S1P receptor, EDG1, is coupled to MAPK in a PTX-sensitive manner in mammalian cells [29,30] and to inhibition of adenylate cyclase in both mammalian cells [33] and Sf9 insect cells [30]. In addition to these observations, we independently found that EDG1 is coupled exclusively via G_i to multiple signalling pathways, including activation of phospholipase C, Ca^{2+} mobilization and inhibition of adenylate cyclase, in mammalian expression systems [31]. Unlike EDG1, we report that AGR16 is coupled largely via PTX-insensitive G-proteins to phospholipase C, Ca^{2+} mobilization, and c-Jun N-terminal kinase (JNK) and p38 MAPKs. When activated with higher concentrations of S1P, AGR16 is coupled via a PTX-sensitive G-protein to the Ras/MAPK pathway.

MATERIALS AND METHODS

Cells

CHO (CHO-K1) cells and K562 cells were obtained from the RIKEN Cell Bank (Tsukuba, Japan) and the Japanese Cancer Research Resources Bank (Tokyo, Japan) respectively, and were grown in Ham's F12 (CHO cells) and RPMI (K562 cells) medium respectively supplemented with 10% (v/v) fetal calf serum (Equitech-Bio, Ingram, TX, U.S.A.), 100 units/ml penicillin and 100 μg/ml streptomycin (Wako Pure Chemicals, Osaka, Japan). At 24 h before each experiment, cells were switched to the respective medium supplemented with 1% (v/v) fetal calf serum.

Measurement of intracellular free Ca^{2+} concentration ($[Ca^{2+}]_i$), inositol phosphate production and cAMP content

$[Ca^{2+}]_i$ was measured as described previously [34,35], except that BSA was not included in the buffer, in fura-2-loaded trypsinized cells using a CAF-110 spectrofluorimeter (Japan Spectroscopy, Inc., Tokyo, Japan), with excitation at 340 and 380 nm and emission at 500 nm.

For measurement of the production of inositol phosphates, cells were prelabelled with 4 μCi/ml *myo*-[2-^{3}H]inositol in Ham's F12 medium supplemented with 1% (v/v) fetal calf serum for 24 h, and stimulated with S1P in the presence of 10 mM LiCl for 30 min [35]. The fraction containing total inositol phosphates was separated as described [34,35] and the radioactivity was quantified by liquid scintillation counting.

For measurement of cellular cAMP content, cells were incubated with or without 0.5 μM forskolin for 5 min in the presence of 0.2 mM 3-isobutyl-1-methylxanthine, and then stimulated with S1P for 5 min. The reaction was terminated by adding HCl (final concentration 0.1 M), and the amount of cAMP in the acid extracts was measured by RIA using a Yamasa cAMP kit (Choshi, Japan) [34].

Plasmids and transfections

Rat full-length AGR16 cDNA (DDBJ/GenBank/EMBL accession no. AB016931) was cloned by hybridization screening of a λgt10 cDNA library made from rat aortic smooth muscle cells [24]. AGR16 cDNA was ligated into the mammalian expression vector pME18S (obtained from Dr. K. Maruyama, Tokyo Medical and Dental College, Tokyo, Japan) at the *Eco*RI site downstream of the SRα promoter. Transfections of cells were carried out by using Lipofectamine (GIBCO-BRL) as described [36]. Stable transfectants were selected with G418 as described [35].

Assays of MAPK, JNK and p38 activities

For measurement of the MAPK activity in transiently transfected cells, CHO cells in 35 mm-diam. dishes were co-transfected with pME18S-Myc-MAPK [36] and either pME18S-[Asn^{17}]Ras ([Asn^{17}]Ras cDNA was obtained from Dr. G. Cooper, Harvard Medical School, Cambridge, MA, U.S.A.) or the empty vector pME18S. The cells were lysed in lysis buffer containing 50 mM Tris (pH 8.0), 1 mM EDTA, 150 mM NaCl, 1 mM Na_3VO_4, 1 mM PMSF, 10 μg/ml each of leupeptin and aprotinin, 0.5% sodium deoxycholate, 0.1% SDS and 1% Nonidet P-40. Myc-tagged MAPK was immunoprecipitated by using a mouse monoclonal anti-(Myc epitope) antibody (clone 9E10). The MAPK activity associated with the immune complex was assayed *in vitro* using myelin basic protein (Sigma) as a substrate, as described [36]. The band shift of p42 ERK was detected by Westen blot analysis of total cell lysate with a mouse monoclonal anti-ERK antibody (clone 03-6600; Zymed Laboratories Inc.) [31,37]. The densities of the bands corresponding to phosphorylated and non-phosphorylated p42 ERKs were quantified using a densitometer (PDI), and the ratio of phosphorylated/(phosphorylated plus non-phosphorylated) bands was calculated for each sample.

For measurement of JNK activity in CHO cells and CHO-AGR16 cells, cells were lysed in lysis buffer containing 25 mM Hepes (pH 7.5), 1% Triton X-100, 0.5% Nonidet P-40, 500 mM NaCl, 50 mM NaF, 5 mM EDTA, 3 mM EGTA, 1 mM Na_3VO_4, 10 μg/ml each of leupeptin and aprotinin, and 1 mM PMSF [36,38]. JNK1 was immunoprecipitated using rabbit polyclonal anti-(JNK1 C-terminus) antibody (Santa Cruz; C-17). The immunoprecipitate was incubated with 30 μl of JNK assay buffer containing 3 μg of glutathione S-transferase (GST)–c-Jun-(5–89) at 30 °C for 30 min, as described [36,38].

For measurement of p38 MAPK activity, cells were lysed in lysis buffer containing 50 mM Tris (pH 8.0), 60 mM β-glycerophosphate, 0.5% Nonidet P-40, 0.2% SDS, 100 mM NaF, 1 mM Na_3VO_4, 2 mM EGTA, 10 μg/ml each of aprotinin and leupeptin, and 0.6 mM PMSF [39]. p38 MAPK was immunoprecipitated using goat polyclonal anti-(p38 C-terminus) antibody (Santa Cruz; C-20-G). The immunoprecipitate was incubated with 30 μl of JNK assay buffer containing 1 μg of GST–ATF2-(1–109) (where ATF2 is activating transcription factor 2) at 30 °C for 30 min. The reaction was terminated and analysed as described for MAPK and JNK [36,38].

Phalloidin staining of stress fibres and microscopy

At 48 h before stimulation with S1P, cells were switched to medium containing 1 % (v/v) fetal calf serum with or without the indicated toxins. Cells were stimulated with S1P, washed with PBS, fixed in 3.7 % formaldehyde in PBS for 10 min, permeabilized with 0.1 % Triton X-100 in PBS for 5 min, and then incubated in a buffer containing 20 mM Hepes (pH 7.2) and 50 mM glycine. For actin localization, cells were incubated with 0.1 μg/ml tetramethylrhodamine B isothiocyanate (TRITC)-conjugated phalloidin (Amersham) for 60 min at room temperature. Cells were viewed on an Olympus microscope, and photographed on Fuji Neopan 400 film.

Phosphorylation of 20 kDa myosin light chain (MLC)

Cells were treated as described for phalloidin staining, lysed in Laemmli SDS sample buffer and analysed by Western blotting using an anti-phospho-MLC antibody [40] and an anti-MLC antibody [41].

[^{32}P]S1P binding

Cells on a 12-well plate were washed with binding medium [RPMI 1640 medium containing 10 mM Hepes (pH 7.4) and incubated in binding medium containing 0.5 nM [^{32}P]S1P (6000 c.p.m./well) in the presence or absence of various concentrations of unlabelled S1P for 150 min at 25 °C [22]. [^{32}P]S1P was prepared enzymically from sphingosine and [γ-^{32}P]ATP using sphingosine kinase obtained from human platelets [42]. The time-course study revealed that [^{32}P]S1P binding to cells became saturated by 150 min. After washing the cells three times with ice-cold binding medium, cell-bound radioactivity was counted. Specific binding was determined by subtracting non-specific binding in the presence of 10 μM S1P from each binding value.

Materials

S1P, SPC and ceramide (C_8)-1-phosphate were obtained from Biomol (Plymouth Meeting, PA, U.S.A.). To examine the purity of S1P and SPC, 3 nmol of each of these lipids was applied to silica gel 60 HPTLC plates (Merck, Darmstadt, Germany), and the plates were developed in butanol/acetic acid/water (3:1:1, by vol.). The bands were identified by primulin staining, and visualized under UV light. The R_f values for S1P and SPC were found to be 0.48 and 0.20 respectively, and no other band was detected. Sphingosine, lysophosphatidylserine (purified from bovine brain), lysophosphatidylcholine (C_{18}), lysophosphatidylethanolamine (C_{18}), ceramide (C_6 and C_{18}), phosphatidic acid (diC_{18}), lysophosphatidic acid (LPA; C_{18}) and glucosylsphingosine were purchased from Sigma. Lysophosphatidylinositol (purified from bovine liver) was purchased from Avanti (Birmingham, AL, U.S.A.). Fura-2 acetoxymethyl ester solution and C3 toxin were purchased from Wako Pure Chemicals. S1P was dissolved in DMSO at 2 mM, divided into aliquots and stored at −80 °C. Other lipids were dissolved in methanol. Final solvent concentrations did not exceed 0.25 %. Rabbit polyclonal anti-MLC antibody and mouse monoclonal anti-phospho-MLC antibody were kindly donated by Dr. Y. Sasaki (Asahi Chemical Industry, Fuji, Japan).

RESULTS

Most of the mammalian cell lines often employed for the expression of exogenous genes respond to even low concentrations (~ 1 nM) of S1P [21], suggesting that they abundantly express endogenous S1P receptor(s). However, we found that CHO cells did not respond to low concentrations of S1P with either an increase in $[Ca^{2+}]_i$ or other responses (see below). Therefore we first employed CHO cells for the analysis of AGR16 functions

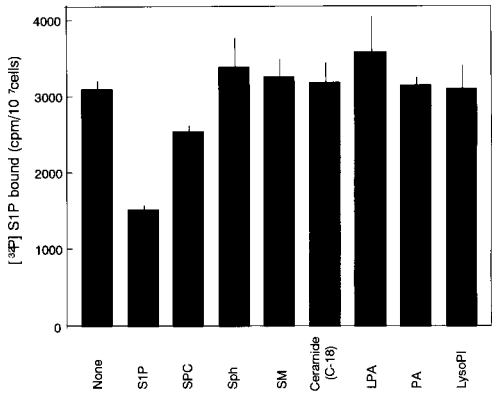

Figure 1 Competition of [^{32}P]S1P binding to intact CHO-AGR16 cells by unlabelled S1P and related lipids

CHO-AGR16 cells were incubated with [^{32}P]S1P in the presence of unlabelled S1P or related lipids (1 μM), as described in the Materials and methods section. Sph, sphingosine; SM, sphingomyelin; PA, phosphatidic acid; LysoPI, lysophosphatidylinositol. Values are mean ± S.E.M. of three determinations.

We established a CHO clone stably expressing the AGR16 receptor (CHO-AGR16). We detected specific binding of [^{32}P]S1P to CHO-AGR16 cells, which was inhibited dose-dependently by the addition of unlabelled S1P with an IC_{50} value of 200 nM. In parental CHO cells, specific binding of [^{32}P]S1P was only 10 % of that observed for CHO-AGR16 cells. We examined competition of [^{32}P]S1P binding to CHO-AGR16 cells by related lipids. SPC, a structurally related sphingolipid, reduced [^{32}P]S1P binding when present at 1 μM (Figure 1). Other related lipids examined, including sphingosine and sphingomyelin, did not inhibit [^{32}P]S1P binding to CHO-AGR16 cells.

We studied the signalling mechanism of AGR16 receptors. We first examined S1P-induced Ca^{2+} mobilization in the transient transfection assay. In CHO cells transiently transfected with the AGR16 expression vector, S1P at 1 nM caused a biphasic, sustained increase in $[Ca^{2+}]_i$ with a peak $[Ca^{2+}]_i$ increment of 122 ± 13 nM {mean ± S.E.M. (n = 3), as evaluated as the average $[Ca^{2+}]_i$ increase in a cell population} (Figure 2A). In the absence of extracellular Ca^{2+} (0 mM Ca^{2+} plus 0.1 mM EGTA), S1P still elicited a transient increase in $[Ca^{2+}]_i$, although the amplitude of the peak $[Ca^{2+}]_i$ increase was diminished compared with that in the presence of extracellular Ca^{2+}, and the sustained plateau phase of the $[Ca^{2+}]_i$ increase was abolished. Thus the activation of AGR16 leads to mobilization of Ca^{2+} from both intra- and extra-cellular pools. SPC at 10 nM also increased $[Ca^{2+}]_i$, whereas sphingosine up to 1 μM did not. In sharp contrast, CHO cells transfected with an empty vector did not respond at all to either S1P or SPC at the concentrations described.

Higher concentrations of S1P (> 10 nM) and SPC (⩾ 500 nM) slightly increased $[Ca^{2+}]_i$ in parental CHO cells, suggesting that these cells express a certain level of endogenous S1P receptors. Human erythroleukaemia K562 cells do not respond to S1P, SPC, LPA or other related lipids at concentrations up to 1 μM with an increase in $[Ca^{2+}]_i$ [43]. In order to examine the dose-dependent Ca^{2+}-mobilizing effects of S1P and related lipids, we established a K562 clone stably expressing AGR16 (K562-

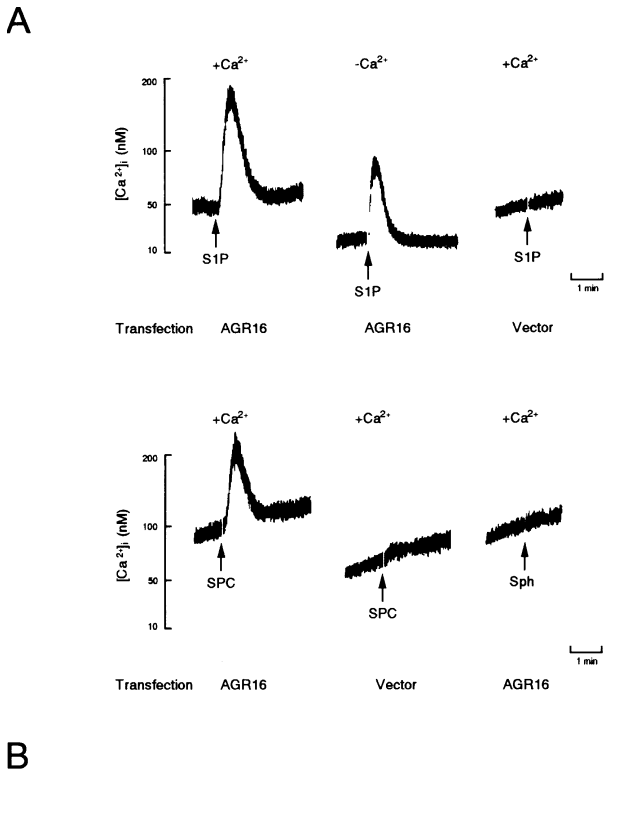

Figure 2 S1P-induced increase in $[Ca^{2+}]_i$ in CHO cells transiently transfected with AGR16, and dose-dependent effects of various lipids on $[Ca^{2+}]_i$ in K562 cells stably expressing AGR16

(**A**) CHO cells that were transiently transfected with either an AGR16 expression vector or an empty vector were loaded with fura-2, and stimulated with 1 nM S1P, 10 nM SPC or 1 μM sphingosine in the presence or absence of extracellular Ca^{2+}. (**B**) K562-AGR16 cells were stimulated with various concentrations of lipids. The maximal increase in $[Ca^{2+}]_i$, with 500 nM S1P, was 90 ± 19 nM ($n = 3$). Values are means $\pm$ S.E.M of three determinations.

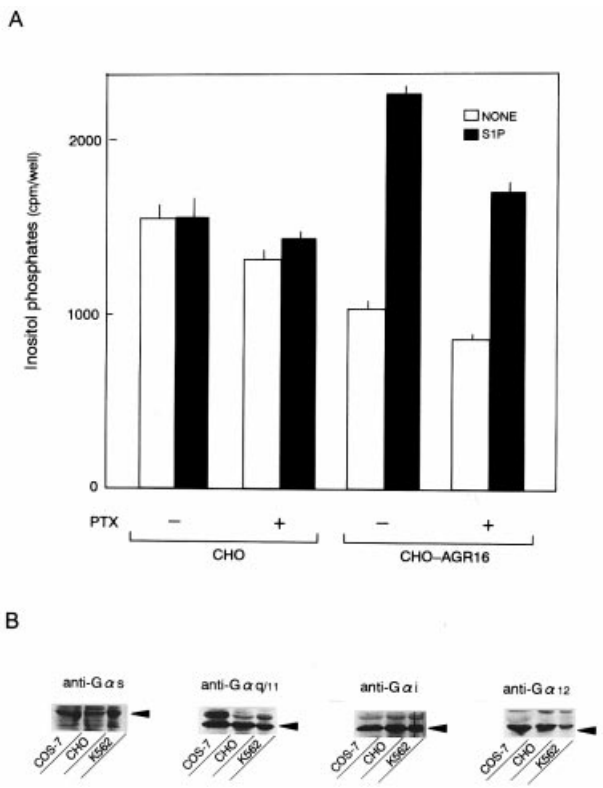

Figure 3 PTX sensitivity of S1P-induced inositol phosphate production in CHO-AGR16 cells, and expression of Gα proteins in CHO and K562 cells

(**A**) Cells prelabelled with *myo*-[2-^{3}H]inositol were pretreated (+) or not (−) with 100 ng/ml PTX for 24 h, and then stimulated with 1 μM S1P for 30 min in the presence of 10 mM LiCl. (**B**) Cell lysates (30 mg of protein per sample) from CHO, K562 or COS-7 cells were separated on a 10% (w/v) polyacrylamide gel and analysed for expression of $G_s\alpha$, $G_{q/11}\alpha$, $G_i\alpha$ and $G_{12}\alpha$ by Western blot analysis using respective specific antibodies.

AGR16). Northern analysis of mRNA from K562-AGR16 cells confirmed the expression of AGR16 mRNA, but not of the mRNAs for the other S1P receptors EDG1 [29–31,33] and EDG3 [32]. In K562-AGR16 cells, S1P increased $[Ca^{2+}]_i$ dose-dependently, with an EC_{50} value of 3 nM; the concentration giving the maximal response was 500 nM (Figure 2B). SPC was a much less potent agonist, with an EC_{50} value of approx. 100 nM. The maximal response obtained with SPC at 500 nM was approx. 60% of that attained with S1P. Other lipids examined, including sphingosine, sphingomyelin, ceramide, ceramide 1-phosphate, glucosylsphingosine, lysophosphatidylinositol, lysophosphatidylcholine, lysophosphatidylethanolamine, lysophosphatidylserine and phosphatidic acid, did not increase $[Ca^{2+}]_i$ in K562-AGR16 cells when present at concentrations up to 1 μM. LPA at 1 μM slightly increased $[Ca^{2+}]_i$ (20% of the maximal response obtained with S1P) in K562-AGR16 cells. However, unlike the SPC-induced $[Ca^{2+}]_i$ response, the LPA-induced $[Ca^{2+}]_i$ increase was not abolished by the prior addition of S1P (1 μM), suggesting that the LPA-induced response was not mediated by AGR16.

Since S1P caused an increase in $[Ca^{2+}]_i$ in CHO cells transiently transfected with AGR16, we examined whether S1P stimulated phospholipase C in CHO-AGR16 cells. We found that S1P stimulated inositol phosphate production by 2.2-fold (Figure 3A). In parental CHO cells, in contrast, S1P failed to induce a detectable increase in inositol phosphate production. Pretreatment of CHO-AGR16 cells with PTX (100 ng/ml for 24 h) inhibited S1P-induced inositol phosphate production by approx. 30% (Figure 3A). Similarly, PTX pretreatment reduced the increase in $[Ca^{2+}]_i$ by 30% (results not shown). Both CHO cells and K562 cells were found to express $G\alpha_i$, $G\alpha_q/_{11}$, $G\alpha_s$ and $G\alpha_{12}$, as evaluated by Western blot analysis (Figure 3B).

We next examined the effect of S1P on MAPK activity and its activation mechanisms in CHO-AGR16 cells. S1P (1 μM) rapidly activated MAPK, with a peak activation at 3 min followed by a gradual decline, as evaluated by detection of the band shift of

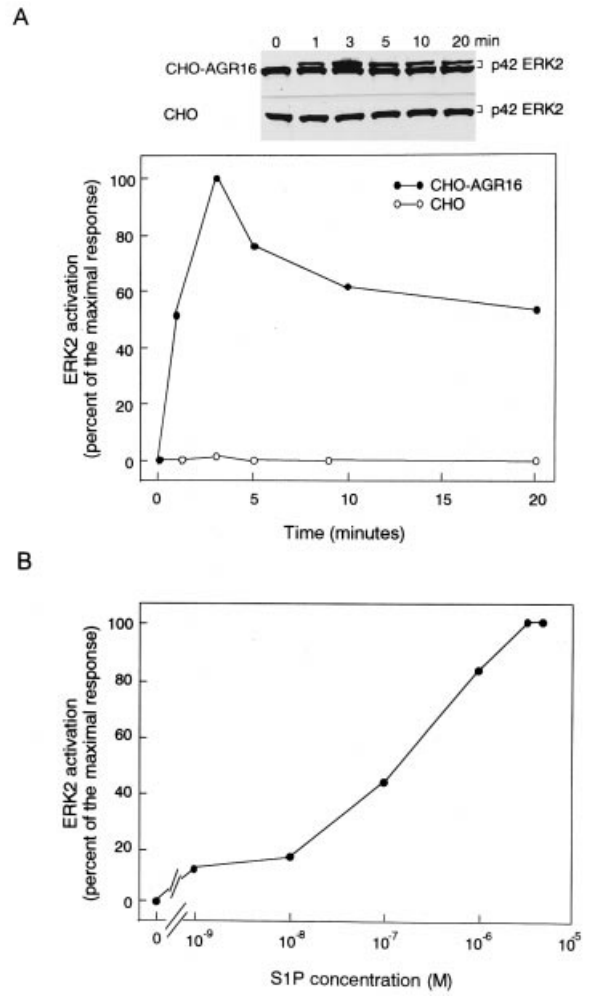

Figure 4 S1P stimulates MAPK activity in CHO-AGR16 cells

(**A**) Time course of S1P-induced MAPK activation. CHO-AGR16 cells and parental CHO cells were stimulated with 1 μM S1P for the indicated time periods. (**B**) Dose-dependent MAPK activation by S1P. CHO-AGR16 cells were stimulated with various concentrations of S1P for 3 min. MAPK activation was evaluated by detection of the band shift of p42 ERK by Western analysis using anti-ERK antibody, as described in the Materials and methods section. Values are means $\pm$ S.E.M of three determinations.

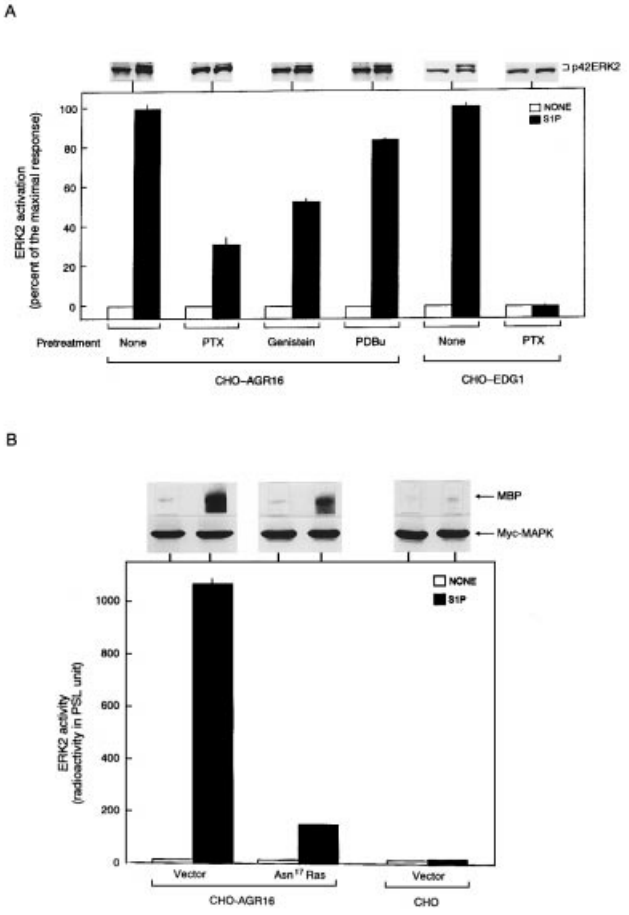

Figure 5 S1P-induced MAPK activation is dependent on Ras and sensitive to PTX and genistein

(**A**) CHO-AGR16 cells and CHO-EDG1 cells (which stably express EDG1) were pretreated with PTX (100 ng/ml for 24 h), genistein (100 μM for 60 min) or phorbol 12,13-dibutyrate (PDBu; 1 μM for 24 h), and stimulated with 1 μM S1P for 3 min. Cell lysates were separated on a 10% (w/v) polyacrylamide gel, followed by Western blotting using an anti-ERK antibody. (**B**) CHO-AGR16 and CHO cells were transiently co-transfected with a Myc-tagged MAPK expression vector and either an [Asn^{17}]H-Ras expression vector or an empty vector, and then stimulated with 1 μM S1P for 3 min. Autoradiograms of myelin basic protein (MBP) and Western blots of Myc–MAPK are shown above the bar graphs. Note that the levels of expression of Myc-tagged MAPK were similar between transfection groups. Values are means $\pm$ S.E.M. of three determinations. Abbreviation: PSL, photostimulated luminescence.

p42 ERK (Figure 4A). S1P-induced MAPK activation increased in a dose-dependent fashion, with an EC_{50} value of approx. 200 nM and a maximally effective concentration of approx. 3 μM (Figure 4B). In parental CHO cells, in contrast, S1P did not activate MAPK detectably. Pretreatment of CHO-AGR16 cells with PTX inhibited S1P-induced MAPK activation strongly (by approx. 70%), as in the case of CHO cells stably expressing EDG1 (CHO-EDG1 cells) (Figure 5A). The addition of genistein, a tyrosine kinase inhibitor, also attenuated S1P-induced ERK activation by 50%. In contrast, down-regulation of PKC by prolonged pretreatment with phorbol 12,13-dibutyrate (1 μM for 24 h) only minimally (16%) inhibited S1P-induced MAPK activation. Down-regulation of PKC totally abolished MAPK activation by acute stimulation with phorbol 12,13-dibutyrate, confirming that down-regulation-sensitive PKC isoforms were effectively depleted (results not shown). We also examined whether S1P-induced AGR16-mediated activation of MAPK was dependent upon Ras. CHO-AGR16 cells were co-transfected with an expression vector for Myc-tagged MAPK and either an expression vector for a dominant-negative form of Ras ([Asn^{17}]H-Ras) or an empty vector. After stimulation with S1P, Myc-tagged MAPK was immunoprecipitated using anti-(Myc epitope) antibodies, followed by measurement of the *in vitro* MAPK activity using myelin basic protein as a substrate. The levels of expression of Myc-tagged MAPK were similar among the transfection groups, as evaluated by Western analysis using the anti-(Myc epitope) antibody (Figure 5B). S1P induced a 25-fold stimulation of MAPK activity in CHO-AGR16 cells, as compared with only a 2-fold increase in parental CHO cells. The expression of [Asn^{17}]H-Ras in CHO-AGR16 cells inhibited S1P-induced MAPK activation by more than 80%, indicating the Ras-dependence of the S1P-induced MAPK activation.

We next examined the coupling of AGR16 to two other members of the MAPK family, JNK and p38 MAPK. S1P at 10 nM caused a rapid and sustained activation of both JNK and

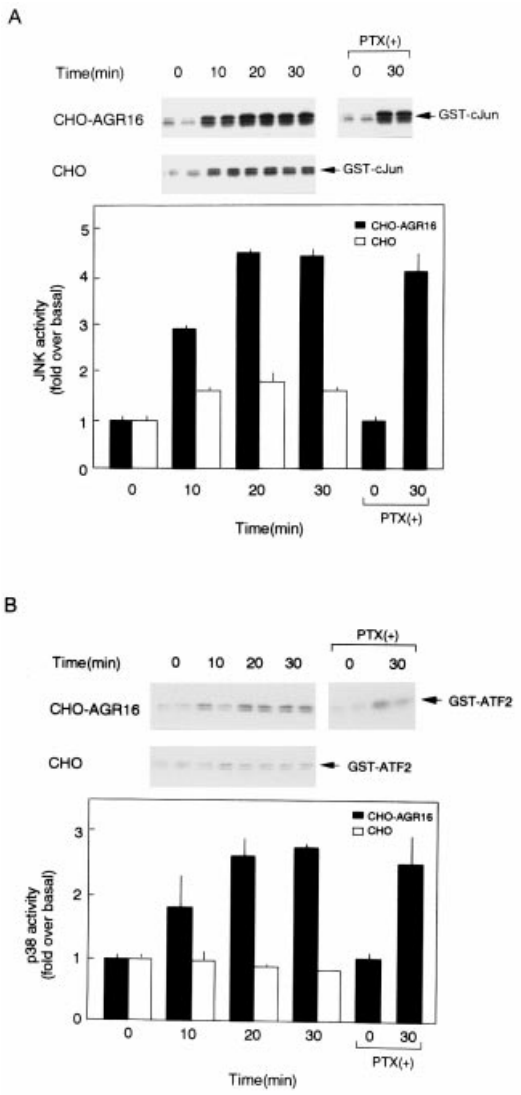

Figure 6 S1P activates JNK and p38 MAPK in a PTX-insensitive manner

Time courses of S1P-induced activation of JNK (**A**) and p38 MAPK (**B**) are shown. CHO-AGR16 cells and CHO cells were stimulated with 10 nM S1P for the indicated time periods. CHO-AGR16 cells on some dishes were pretreated with 100 ng/ml PTX for 24 h. Autoradiograms are shown in the upper panels. JNK1 and p38 MAPK were immunoprecipitated by employing specific antibodies, and the immune complex kinase assay was performed as described in the Materials and methods section, using as substrates GST–c-Jun-(5–89) for JNK and GST–ATF2-(1–109) for p38. Values are means ± S.E.M. of three determinations, and are expressed relative to the activity in cells at time zero, which was given an arbitrary value of 1.

p38 in CHO-AGR16 cells (Figure 6). JNK activity had increased significantly over the basal value by 10 min, and reached a maximal value of 4.5-fold at 20 min (Figure 6A). The time course of the activation of p38 was similar to that of JNK (Figure 6B). In parental CHO cells, in contrast, S1P only activated JNK slightly (1.5-fold), and did not activate p38 MAPK over the basal unstimulated value. The S1P-induced activation of both JNK and p38 in CHO-AGR16 cells increased dose-dependently, and became maximal at 100 nM S1P (results not shown). The S1P-induced, AGR16-mediated activation of both JNK and p38 MAPK was entirely insensitive to PTX pretreatment (100 ng/ml for 24 h) (Figures 6A and 6B).

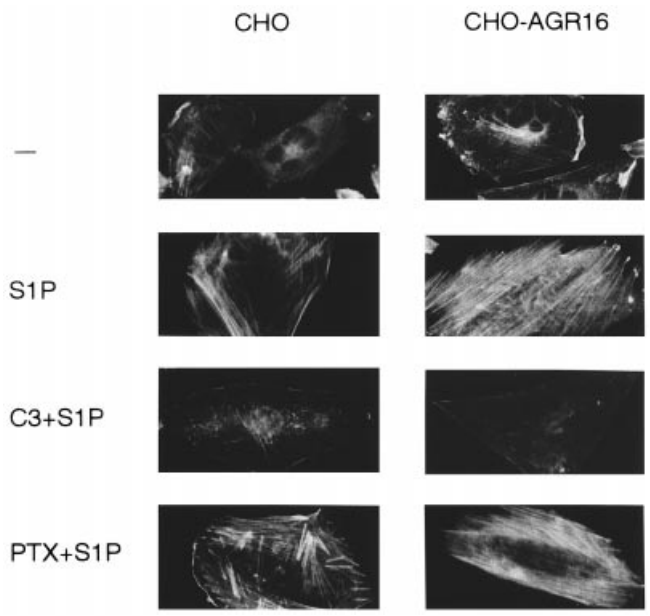

Figure 7 S1P induces stress-fibre formation in CHO-AGR16 cells in a Rho-dependent manner

CHO-AGR16 cells and CHO cells were pretreated with either PTX (100 ng/ml for 24 h) or C3 (20 μg/ml for 48 h), or were left untreated, and were then stimulated with 10 nM S1P for 10 min. Cells were fixed and stained with tetramethylrhodamine B isothiocyanate (TRITC)-conjugated phalloidin for actin stress-fibre localization.

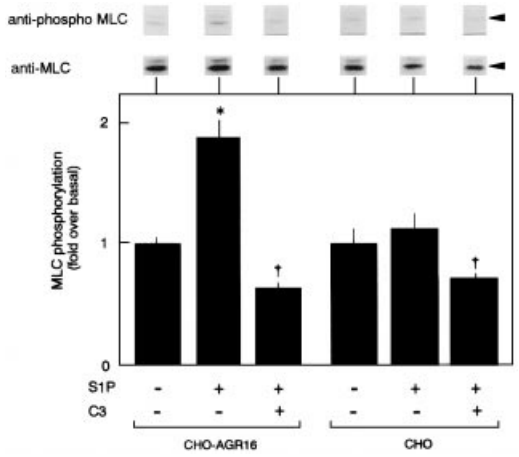

Figure 8 S1P induces an increase in MLC phosphorylation in CHO-AGR16 cells in a Rho-dependent manner

CHO-AGR16 cells and CHO cells were pretreated and stimulated as described in the legend to Figure 7. The cells were solubilized in Laemmli SDS sample buffer and analysed by Western blotting using anti-phospho-MLC antibody or anti-MLC antibody. The density of bands was quantified by densitometry using a densitometer (PDI). Values are means ± S.E.M. of three determinations, and are expressed relative to the value in non-stimulated cells, which was given an arbitrary value of 1. * and † denote statistically significant differences ($P < 0.05$) compared with the untreated group and the S1P-treated group respectively.

We also explored whether AGR16 is coupled to Rho-dependent signalling pathways, by examining the effect of S1P on stress-fibre formation in CHO-AGR16 cells. Stimulation of CHO-AGR16 cells with S1P (10 nM) led to the formation of stress fibres (Figure 7). Pretreatment of CHO-AGR16 cells with

Table 1 S1P increases cellular cAMP content in CHO-AGR16 cells

Cells were preincubated with or without forskolin (0.5 μM) for 5 min, and then stimulated with S1P (1 μM) for 5 min in the presence of 0.2 mM 3-isobutyl-1-methylxanthine. Cellular cAMP content was determined by radioimmunoassay. Results are means ± S.E.M. of three determinations. * and † indicate statistically significant effects of S1P treatment compared with untreated cells and forskolin-treated cells respectively.

Cells	Stimulation	cAMP content (pmol/well)
CHO	None	0.83 ± 0.01
	S1P	0.90 ± 0.07
	Forskolin	9.07 ± 0.77
	Forskolin + S1P	7.52 ± 0.64
CHO-AGR16	None	0.84 ± 0.11
	S1P	4.83 ± 0.36*
	Forskolin	4.71 ± 0.49
	Forskolin + S1P	11.62 ± 0.32†

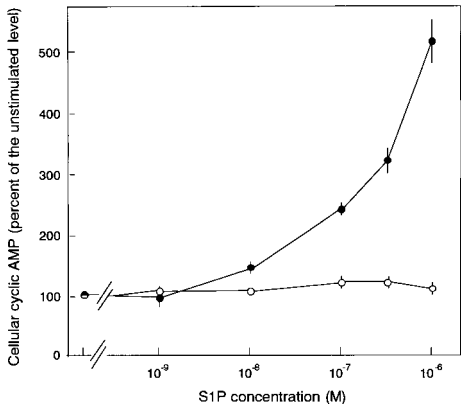

Figure 9 S1P increases cellular cAMP content in a dose-dependent manner

CHO-AGR16 cells (●) and CHO cells (○) were stimulated with various concentrations of S1P in the presence of 0.2 mM 3-isobutyl-1-methylxanthine. Cellular cAMP contents were determined by radioimmunoassay. Results are means ± S.E.M. of three determinations.

C3 toxin (20 μg/ml for 48 h) completely abolished S1P-induced stress-fibre formation, but PTX pretreatment had no effect. In parental CHO cells, S1P induced stress-fibre formation only weakly. We also examined whether S1P caused an increase in MLC phosphorylation, which is thought to underlie S1P-induced stress-fibre formation [44,45], in a Rho-dependent manner. S1P increased MLC phosphorylation [as evaluated by Western blot analysis using an anti-phospho-MLC antibody which specifically recognizes monophosphorylated (Ser^{19}) MLC] in CHO-AGR16 cells, but not in CHO cells (Figure 8). Pretreatment of the cells with C3 toxin abolished the S1P-induced increase in MLC phosphorylation. Total amounts of MLC, as evaluated by anti-MLC immunoblotting, were similar among cells treated in various ways.

Finally, we examined how S1P affects the cellular cAMP content via AGR16 receptors. In CHO-AGR16 cells, S1P (1 μM) caused a 6-fold increase in the cellular cAMP content (Table 1). In forskolin-stimulated CHO-AGR16 cells, S1P caused a further 2.5-fold increase in the cellular cAMP level. In contrast, S1P did not change the cellular cAMP content in parental CHO cells. The stimulatory effect of S1P on the cellular cAMP content in CHO-AGR16 cells was dose-dependent (Figure 9).

DISCUSSION

In the present study, we functionally characterized the putative S1P receptor AGR16 by expressing it in two mammalian cell lines, CHO and K562. Many of cell lines usually employed for the expression of exogenous genes, including COS, NIH 3T3 and HEK293 cells, respond vigorously to S1P [21]. In contrast, CHO cells respond to S1P exclusively at high doses, with only a slight increase in $[Ca^{2+}]_i$, and K562 cells do not respond at all to S1P or related lipids, even at high doses [43]. By employing mammalian expression systems with a very low or no background of responses to S1P, we here establish that AGR16 is a functional receptor with a substantially high selectivity for S1P, which is coupled via both PTX-sensitive and -insensitive G-proteins to multiple signalling pathways.

We first demonstrated in the present study that CHO-AGR16 cells bind [^{32}P]S1P. Among a number of related lipids, including LPA, only SPC reduced binding of [^{32}P]S1P to CHO-AGR16 cells (Figure 1). Thus AGR16 receptors are selective for S1P and SPC, contrasting with the two other members of EDG family, EDG2 and EDG4, which are responsive to LPA, but not to S1P [46–49]. Consistent with this, detailed examination of the Ca^{2+}-mobilizing potencies of various lipids in K562-AGR16 cells revealed that S1P, and less potently SPC, increase $[Ca^{2+}]_i$ (Figure 2B). LPA induces a slight increase in $[Ca^{2+}]_i$ in K562-AGR16 cells. However, this response is probably mediated by endogenous LPA receptors [42–45], since the response to LPA is not abolished by the prior addition of S1P.

The S1P-induced activation of phospholipase C is only partially (30%) inhibited by PTX pretreatment (Figure 3A). The AGR16-induced $[Ca^{2+}]_i$ increase is also only partially inhibited by PTX. Thus AGR16 triggers phospholipase C activation with Ca^{2+} mobilization primarily via a PTX-insensitive G-protein, most likely of the G_q class. This contrasts sharply with the case of EDG1, the first S1P receptor to be identified [29,30], which we found recently to be coupled exclusively via G_i to phospholipase C activation and Ca^{2+} mobilization [31]. On the other hand, AGR16 mediates MAPK activation largely via a PTX-sensitive G-protein, most likely of the G_i class (Figure 5A). AGR16-mediated MAPK activation is dependent on Ras and is sensitive to genistein, but not to PKC down-regulation (Figure 5A). These modes of MAPK activation are similar to those reported previously for G_i-coupled MAPK activation by other heptahelical receptors. Interestingly, the EC_{50} value (200 nM) for S1P-induced MAPK activation is as much as 70-fold higher than that for the S1P-induced $[Ca^{2+}]_i$ increase (compare Figures 2 and 4B). Thus the coupling of AGR16 via G_i to MAPK appears to be much less efficient than the coupling via G_q to Ca^{2+} mobilization. This characteristic of AGR16 again clearly differs from EDG1, which is efficiently coupled via G_i to MAPK [29–31].

The present study also shows that AGR16 is linked to at least three additional signalling pathways, i.e. JNK, p38 MAPK and the Rho-dependent pathway, through PTX-insensitive mechanisms. In contrast with AGR16-mediated MAPK activation (Figures 4 and 5), a low concentration of S1P (10 nM) effectively activates both JNK and p38 MAPK in CHO-AGR16 cells in a manner totally insensitive to PTX (Figure 6). Previous studies showed that both the α and $\beta\gamma$ subunits of several classes of heterotrimeric G-proteins, including G_i, G_q and $G_{12/13}$, could mediate the activation of JNK [36,50–52] and p38 MAPK [50,51]. Since the S1P-induced activation of JNK and p38

MAPK is PTX-insensitive, G_q and $G_{12/13}$ are likely candidates for G-proteins that mediate the activation of these kinases. Identification of the exact heterotrimeric G-protein(s) responsible for the activation of JNK and p38 MAPK awaits further investigation.

The activation of AGR16 also promotes stress-fibre formation and MLC phosphorylation (Figures 7 and 8). Botulinum C3 toxin, which specifically ADP-ribosylates and inactivates Rho [53], abolishes S1P-induced stress-fibre formation and the increase in MLC phosphorylation, indicating that AGR16 mediates these responses via Rho. It has been demonstrated that actin–myosin-interaction-driven contraction is probably the driving force that promotes the Rho-mediated formation of stress fibres and focal adhesions [44]. Contractility in non-muscle cells is regulated by the phosphorylation status of MLC [45]. An S1P-induced, Rho-dependent increase in MLC phosphorylation is most probably mediated by a recently identified Rho-associated protein kinase, called Rho kinase/ROK/ROCK [54]. A recent study [52] showed that the PTX-insensitive G-protein $G_{12/13}$ is linked to Rho-dependent signalling pathways. Very recently, it was demonstrated that the p115 Rho guanine nucleotide exchange factor interacts with $G\alpha_{12}$ and $G\alpha_{13}$, and that $G\alpha_{13}$ directly stimulates its guanine nucleotide exchange activity [55,56]. Consistent with this, AGR16-mediated stress-fibre formation is PTX-insensitive. It is of note that PTX-insensitive, Rho-mediated gene expression has recently been reported for EDG1 as well [29]. Thus AGR16 appears to be linked to the activation of multiple low-molecular-mass G-proteins, including Ras and Rho, via distinct heterotrimeric G-proteins

The present study also shows that stimulation of AGR16 causes an increase in the cellular cAMP content (Table 1 and Figure 9). Our observation is consistent with a previous report [8] that S1P induced an increase in the cellular cAMP content in human vascular smooth muscle cells, but contrasts with the case of EDG1, which was shown to mediate a decrease in the cellular cAMP content [30,31,33]. Although we did not examine the mechanisms of the AGR16-mediated increase in cellular cAMP, there are several possibilities. First, AGR16 may be weakly coupled to G_s, leading to the activation of adenylate cyclase. Secondly, activation of AGR16 may stimulate the generation and release of chemical mediators such as prostaglandins, which then activate their own G_s-coupled receptors in an autocrine/paracrine fashion. Thirdly, the AGR16-mediated $[Ca^{2+}]_i$ increase and PKC activation may alter the activities of adenylate cyclase and/or cAMP phosphodiesterase, leading to an increase in the cellular cAMP content. These possibilities remain to be elucidated.

The present study, together with recent observations [29–31,33], reveal that AGR16 and EDG1 are both high-affinity S1P receptors, but each has distinct signalling characteristics. The recent report by An et al. [32] demonstrates that EDG3 also functions as a receptor for S1P. At present, however, the agonist specificity and signalling mechanisms of EDG3 are incompletely understood. A more complete exploration of the S1P receptor family should provide a better understanding of the lysosphingolipid signalling system.

We thank R. Suzuki for excellent secretarial assistance. This work was supported by grants from the Ministry of Education, Science and Culture of Japan.

REFERENCES

1 Spiegel, S., Olivera, A. and Carlson, R. U. (1993) Adv. Lipid Res. **26**, 105–129
2 Hannun, Y. A. and Linardic, C. M. (1993) Biochim. Biophys. Acta **1154**, 223–236
3 Spiegel, S. and Merrill, A. M. (1996) FASEB J. **10**, 1388–1397
4 Meyer Zu Heringdorf, D., van Koppen, C. J. and Jakobs, K. H. (1997) FEBS Lett **410**, 34–38
5 Desai, N. N. and Spiegel, S. (1991) Biochem. Biophys. Res. Commun. **181**, 361–366
6 Zhang, H., Desai, N. N., Olivera, A., Seki, T., Brooker, G. and Spiegel, S. (1991) J. Cell Biol. **114**, 155–167
7 Sadahira, Y., Ruan, F., Hakomori, S. and Igarashi, Y. (1992) Proc. Natl. Acad. Sci U.S.A. **89**, 9686–9690
8 Bornfeldt, K. E., Graves, L. M., Raines, E. W., Igarashi, Y., Wayman, G., Yamamura, S., Yatomi, Y., Sidhu, J. S., Krebs, E. G., Hakomori, S. and Ross, R (1995) J. Cell Biol. **130**, 193–206
9 Postma, F. R., Jalink, K., Hengeveld, T. and Moolenaar, W. H. (1996) EMBO J. **15**, 2388–2395
10 Yatomi, Y., Ruan, F., Hakomori, S. and Igarashi, Y. (1995) Blood **86**, 193–202
11 Ghosh, T. K., Bian, J. and Gill, D. L. (1994) J. Biol. Chem. **269**, 22628–22635
12 Mattie, M., Brooker, G. and Spiegel, S. (1994) J. Biol. Chem. **269**, 3181–3188
13 Meyer zu Heringdorf, D., Lass, H., Alemany, R., Laser, K. T., Neumann, E., Zhang, C., Schmidt, M., Rauen, U., Jakobs, K. H. and van Koppen, C. J. (1998) EMBO J. **17**, 2830–2837
14 Choi, O. H., Kim, J. M. and Kinet, J. P. (1996) Nature (London) **380**, 634–636
15 Olivera, A. and Spiegel, S. (1993) Nature (London) **365**, 557–560
16 Goodemote, K. A., Mattie, M. E., Berger, A. and Spiegel, S. (1996) J. Biol. Chem. **270**, 10272–10277
17 Chao, C. P., Laulederkind, S. J. F. and Ballou, L. R. (1994) J. Biol. Chem. **269**, 5849–5856
18 Wu, J., Spigel, S. and Sturgill, T. W. (1995) J. Biol. Chem. **270**, 11484–11488
19 Seufferlein, T. and Rozengurt, E. (1995) J. Biol. Chem. **270**, 24334–24342
20 Büneman, M., Liliom, K., Brandt, B. K., Pott, L., Tseng, J. L., Desiderio, D. M., Sun, G., Miller, D. and Tigyi, G. (1996) EMBO J. **15**, 5527–5534
21 van Koppen, C. J., Meyer zu Heringdorf, D., Laser, K. T., Zhang, C., Jabobs, K H., Bünemann, M. and Pott, L. (1996) J. Biol. Chem. **271**, 2082–2087
22 Yatomi, Y., Yamamura, S., Ruan, F. and Igarashi, Y. (1997) J. Biol. Chem. **272**, 5291–5297
23 Yatomi, Y., Igarashi, T., Yang, L., Hisano, N., Qi, R., Asazuma, N., Satoh, K., Ozaki, Y. and Kume, S. (1997) J. Biochem. (Tokyo) **121**, 969–973
24 Okazaki, H., Ishizaka, N., Sakurai, T., Kurokawa, K., Goto, K., Kumada, M. and Takuwa, Y. (1993) Biochem. Biophys. Res. Commun. **190**, 1104–1109
25 Maclennan, A. J., Browe, C. S., Gaskin, A. A., Lado, D. C. and Shaw, G. (1994) Mol. Cell. Neurosci. **5**, 201–209
26 Hla, T. and Maciag, T. (1990) J. Biol. Chem. **265**, 9308–9313
27 Masana, M. I., Brown, R. C., Pu, H., Gurney, M. E. and Dubocovich, M. L. (1995) Receptors Channels **3**, 255–262
28 Yamaguchi, F., Tokuda, M., Hatase, O. and Brenner, S. (1996) Biochem. Biophys. Res. Commun. **227**, 608–614
29 Lee, M., Van Brocklyn, J. R., Thangada, S., Liu, C. H., Hand, A. R., Menzeleev, R., Spiegel, S. and Hla, T. (1998) Science **279**, 1552–1555
30 Zondag, G. C. M., Postma, F. R., Van Etten, I., Verlaan, I. and Moolenaar, W. H. (1998) Biochem. J. **330**, 605–609
31 Okamoto, H., Takuwa, N., Gonda, K., Okazaki, H., Chang, K., Yatomi, Y., Shigematsu, H. and Takuwa, Y. (1998) J. Biol. Chem. **273**, 27104–27110
32 An, S., Bleu, T., Huang, W., Hallmark, O. G., Coughlin, S. R. and Goetzl, E. J. (1997) FEBS Lett. **417**, 279–282
33 Van Brocklyn, J. R., Lee, M. J., Menzeleev, R., Olivera, A., Edsall, L., Cuvillier, O., Thomas, D. M., Coopman, P. J. P., Thangada, S., Liu, C. J., et al. (1998) J. Cell Biol. **142**, 229–240
34 Takuwa, Y., Kasuya, T., Takuwa, N., Kudo, M., Yanagisawa, M., Goto, K. Masaki, T. and Yamashita, K. (1990) J. Clin. Invest. **85**, 653–658
35 Chang, K., Hanaoka, K., Kumada, M. and Takuwa, Y. (1995) J. Biol. Chem. **270**, 26152–26158
36 Mitsui, H., Takuwa, N., Kurokawa K., Exton, J. H. and Takuwa, Y. (1997) J. Biol. Chem. **272**, 4904–4910
37 Takuwa, N. and Takuwa, Y. (1997) Mol. Cell. Biol. **17**, 5348–5358
38 Hamada, K., Takuwa, N., Yokoyama, K. and Takuwa, Y. (1998) J. Biol. Chem. **273**, 6334–6340
39 Mitsui, H., Maruyama, T., Kimura, S. and Takuwa, Y. (1998) Hepatology **27**, 1362–1367
40 Sakurada, K., Ikuhara, T., Seto, M. and Sasaki, T. (1994) J. Biochem. (Tokyo) **115**, 18–21
41 Sasaki, Y., Sasaki, Y., Kanno, K. and Hidaka, H. (1987) Am. J. Physiol. **253**, C71–C78
42 Yatomi, Y., Ruan, F., Megidish, T., Toyokuni, T. Hakomori, S. and Igarashi, Y. (1996) Biochemistry **35**, 626–633
43 Durieux, M. E., Carlisle, S. J., Salafranca, M. N. and Lynch, K. R. (1993) Am. J. Physiol. **264**, C1360–C1364
44 Chrzanowska-Wodnicka, M. and Burridge, K. (1996) J. Cell Biol. **133**, 1403–1415

45 Tan, J. L., Ravid, S. and Spudich, J. A. (1992) Annu. Rev. Biochem. **61**, 721–759
46 Hecht, J. H., Weiner, J. A., Post, S. R. and Chun, J. (1996) J. Cell Biol. **135**, 1071–1083
47 An, S., Bleu, T., Hallmark, O. G. and Goetzl, E. J. (1998) J. Biol. Chem. **273**, 7906–7910
48 Fukushima, N., Kimura, Y. and Chun, J. (1998) Proc. Natl. Acad. Sci. U.S.A. **95**, 6151–6156
49 Erickson, J. R., Wa, J. J., Goddard, J. G., Tigyi, G., Kawanishi, K., Tomei, L. D. and Kiefer, M. C. (1998) J. Biol. Chem. **273**, 1506–1510
50 Collins, L. R., Minden, A., Karin, M. and Brown, J. H. (1996) J. Biol. Chem. **271**, 17349–17358
51 Yamauchi, J., Nagao, M., Kaziro, Y. and Itoh, H. (1997) J. Biol. Chem. **272**, 27771–27777
52 Buhl, A. M., Johnson, N. L., Dhanasekaran, N. and Johnson, G. L. (1995) J. Biol. Chem. **270**, 24631–24634
53 Kikuchi, A., Yamamoto, K., Fujita, T. and Takai, Y. (1988) J. Biol. Chem. **263**, 16303–16308
54 Lim, L., Manser, E., Lewng, T. and Hall, C. (1996) Eur. J. Biochem. **242**, 171–185
55 Kozasa, T., Jiang, X., Hart, M. J., Sternweis, P. M., Singer, W. D., Gilman, A. G., Bollag, G. and Sternweis, P. C. (1998) Science **280**, 2109–2111
56 Hart, M. J., Jiang, X., Kozasa, T., Roscoe, W., Singer, W. D., Gilman, A. G., Sternweis, P. C. and Bollag, G. (1998) Science **280**, 2112–2114

Received 29 June 1998/21 September 1998; accepted 26 October 1998